CRYSTAL GROWTH & DESIGN

pubs.acs.org/crystal

Article

First Experimental Evidences of the Ferroelectric Nature of Struvite

Jolanta Prywer,* Davide Delmonte, Massimo Solzi, Francesco Cugini, Krystian Roleder, Andrzej Soszyński, Agnieszka Ciżman, and Jan K. Zaręba

Cite This: *Cryst. Growth Des.* 2020, 20, 4454−4460

Read Online

ACCESS | Metrics & More | Article Recommendations

ABSTRACT: Struvite ($MgNH_4PO_4{\cdot}6H_2O$) is a mineral first identified in 1845. It is tested for several reasons: (1) it is a problem in liquid wastewater treatment plants; (2) on the other hand, it is recovered from this wastewater because of phosphorus, magnesium, and nitrogen; (3) it is the main component of infectious urinary stones. In this paper, we present the first experimental evidences of the ferroelectric nature of struvite at room temperature. Struvite shows a hysteresis loop and spontaneous electric polarization that can be reversed by an application of an external electric field. The measured value of residual polarization of struvite is equal to 0.95 $\mu C/cm^2$. We also report observations of the ferroelectric domains in struvite using birefringence imaging technique. The non-centrosymmetry of the crystal lattice is confirmed with the use of the Kurtz−Perry powder test. The second harmonic generation response for struvite in relation to that of potassium dihydrogen phosphate is 0.36. We suggest that ferroelectric properties for struvite, in particular, spontaneous polarization, can have a significant impact on the behavior of struvite in aqueous solutions, such as liquid wastewater or urine.

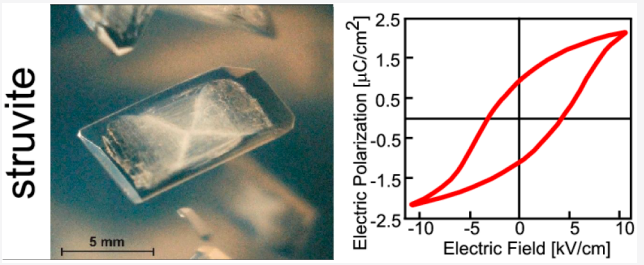

1. INTRODUCTION

The phenomenon of ferroelectricity (FE) consists of the existence of a spontaneous electric polarization of the crystal, whose direction can be switched by an external electric field. The dependence of the resultant (macroscopic) polarization on the electric field has a characteristic loop shape, called the ferroelectric hysteresis loop. The ferroelectric state is the result of a phase change at the Curie temperature T_C, during which a permanent dipole moment, related to the spontaneous polarization, appears (below T_C) or disappears (above T_C). Below T_C crystal is divided into areas called ferroelectric domains, differing in the direction of polarization. Ferroelectrics are a subgroup of pyroelectrics, but all ferroelectrics are piezoelectrics. FE was discovered in 1920 while studying the dielectric properties of Rochelle salt (potassium sodium tartrate tetrahydrate), $NaKC_4H_4O_6{\cdot}4H_2O$, a crystal with a polar orthorhombic structure.[1−3] The second ferroelectric material, discovered after several years, was potassium dihydrogen phosphate, KH_2PO_4 (KDP).[4] The ferroelectric properties of the third very important material, barium titanate, $BaTiO_3$, were discovered in the 1940s.[5] At present, we know of several hundred ferroelectric materials.[6] These materials are still intensively studied for a better knowledge and understanding of the ferroelectric phenomenon as well as to optimize these materials for specific applications.

FE also occurs in minerals, although in the case of minerals this is not a common phenomenon. A review article[7] indicates only 44 minerals exhibiting FE, due to strong symmetry constraints which the unit cell has to respect according to the Landau theory.[8] Struvite, the magnesium ammonium phosphate hexahydrate $MgNH_4PO_4{\cdot}6H_2O$ that is the subject of the research presented in this article, is also a mineral. For the first time, it was identified in sewers in the church of St. Nicholas in Hamburg, Germany.[9] This mineral was named a struvite in honor of Heinrich Christoph Gottfried Struve (1772−1851), the Russian consul of Hamburg, who performed this function at the time when this mineral was discovered.[10] Today, we know that struvite is a fascinating inorganic material, and its crystallization has been widely studied in recent years for several reasons.

First of all, struvite often represents a problem in wastewater treatment plants because it easily precipitates at certain locations, which can lead to sewage pipes clogging.[11−16] Most often, struvite is formed in places with high turbulence; these can be pipe elbows, valves, or aeration units. In places with high turbulence, carbon dioxide is released. This is the so-called degassing process, which in turn leads to an increase in pH, and a higher pH promotes the formation of struvite.

Received: February 27, 2020
Revised: April 8, 2020
Published: April 9, 2020

https://dx.doi.org/10.1021/acs.cgd.0c00260
Cryst. Growth Des. 2020, 20, 4454−4460

Under favorable conditions, struvite can build up quickly, leading to a pipe obstruction.

On the other hand, struvite is the main compound recovered from wastewater because it is a source of phosphorus, nitrogen, and magnesium and can therefore be converted into a useful fertilizer containing these elements (for example, refs 17−19). Struvite recovery from wastewater is particularly important due to phosphorus.[12,13,17] In addition to nitrogen and potassium, phosphorus is one of the most important elements necessary for plant life. Phosphorus deficiency causes various undesirable effects on plants, for example, slowing their growth. Therefore, phosphorus recovery from wastewater, in particular, from struvite, is very important.

The third and most important reason why struvite has been the subject of research in recent years is the fact that it is the main component of so-called infectious urinary stones. The formation of these stones is associated with urinary tract infection caused by urease-positive bacteria, mainly of the *Proteus* species.[20−26] Urease is a bacterial enzyme catalyzing the hydrolysis of urea, a natural component of urine. Hydrolysis of urea, consequently, leads to the formation of ammonia. Urea decomposition also initiates a cascade of chemical reactions leading to an increase in urine pH and an increase in the concentration of NH_4^+, CO_3^{2-}, and PO_4^{3-} ions. These ions together with magnesium ions Mg^{2+} present in urine lead to crystallization of struvite.[22,27,28] Infectious urinary stones constitute up to 30% of all urinary stones.[29,30] Studies show that in highly developed countries the number of people diagnosed with infectious urinary stones is steadily increasing, which indicates that this type of stones is a social problem.

According to the presented literature, struvite is an interesting inorganic material studied for various reasons.

The purpose of the research presented in this article is to examine the ferroelectric properties of this crystal. To our knowledge, there are no literature reports on the ferroelectric properties of struvite, so our research presented in this article is the first study on this subject. We undertake this research mainly because struvite is the main component of infectious urinary stones. In this paper, we put forward a hypothesis that ferroelectric properties, and thus spontaneous polarization, may for example affect the different capture of admixtures on opposite crystal faces perpendicular to the polarization vector. Thus, the examination of these properties may indicate potential ways of dealing with struvite to, for example, inhibit the nucleation and/or growth of struvite in the urinary tract. Additionally, the ferroelectric properties, and in particular the existence of spontaneous polarization, can affect the value of the zeta potential of struvite and, consequently, the aggregation of small struvite crystals, which leads to the formation of large stone. The above phenomena such as nucleation or aggregation of struvite crystals have been studying for years, but we still do not have full knowledge about them.

2. MATERIALS AND METHODS

2.1. Struvite Crystals Growth from Gel Medium. To study the ferroelectric properties, and in particular to measure the hysteresis loop, struvite crystals in the form of a flat plate with specific sizes were necessary. We have grown such crystals in a metasilicate gel environment using a single diffusion gel growth technique. All reagent-grade purity chemicals used were purchased from Sigma-Aldrich. For the preparation of the gel, we used anhydrous sodium metasilicate (Na_2SiO_3; SMS), ammonium dihydrogen phosphate ($NH_4H_2PO_4$; ADP), and magnesium acetate tetrahydrate ($(CH_3COO)_2Mg{\cdot}4H_2O$). Chemicals were dissolved in distilled water. A 0.5 M aqueous ADP solution and 1.07 specific gravity SMS solution were mixed together in appropriate amounts to obtain a pH of 7.0. The mixture prepared in this way was poured into 19 cm long tubes with a diameter of 3 cm and allowed to gel for 24 h. After gelation, 25 mL of 1 M magnesium acetate tetrahydrate was gently poured onto the surface of the newly formed gel in test tubes and closed with a lid. The crystal growth usually lasted for 3−4 weeks. After this time, struvite crystals were observed in the form of rectangular platelets about 1 cm long along the *b* axis. A more detailed description can be found in ref 31. Growth conditions were intentionally selected to obtain crystals of this shape and size, since such crystals are desirable for testing ferroelectric properties, and in particular for measuring hysteresis loop.

2.2. Hysteresis Loop Measurement. FE characterization was performed at room temperature by means of a TF Analyzer 2000E system, produced by AiXACcT GmbH, equipped with the AixACcT ferroelectric module and expanded by a TREK 220 high-voltage amplifier, allowing to us characterize also bulk samples. The sample preparation was carried out by preparing a planar plate capacitor circuit through the metallization of thin and large struvite crystals (such as the one in Figure 1) obtained by painting both surfaces

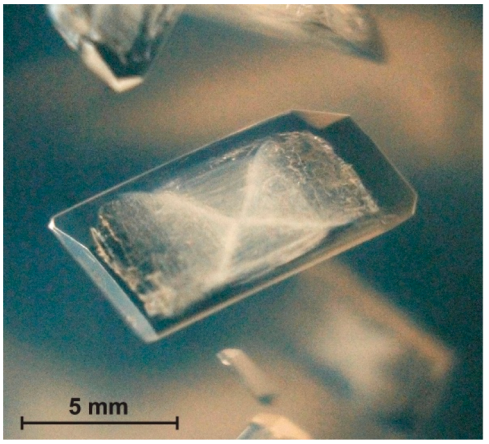

Figure 1. Struvite crystal in a metasilicate gel.

perpendicular to the *z* axis with a thin layer of conductive silver paste (ranging approximately from 20 to 50 μm of thickness) contacted with two 100 μm-diameter copper wires and then put into the gel solution to prevent the phase degradation until the measurement took place. The ferroelectric properties investigation was performed utilizing the dynamic hysteresis measurement (DHM) protocol (which is described in ref 32), by exciting the system with 0.1−5 kHz triangle voltage pulses with amplitudes varying from 20 to 1200 V.

2.3. Second Harmonic Generation Studies. The second harmonic generation (SHG) method was used to confirm the non-centrosymmetricity of struvite, which is necessary for the existence of ferroelectric properties.

The assessment of SHG efficiency of struvite was performed with the use of the Kurtz−Perry technique. Potassium dihydrogen phosphate (KDP) was used as an SHG reference.[33,34] Generally, the Kurtz−Perry technique necessitates the use of crystalline powders of graded particle sizes, in order to preserve the reproducibility of the results. Hence, prior to measurements, the single crystals of struvite and KDP were crushed with a spatula and sieved through a mini-sieve set (Aldrich), collecting a microcrystal size fraction of 125−177 μm. Next, size-graded samples of struvite and KDP were fixed between microscope glass slides (forming tightly packed layers), sealed, and mounted to a holder. The Kurtz−Perry test was performed at 293 K.

The laser radiation was delivered from a Quantronix Integra-C regenerative amplifier operating at 800 nm, pulse duration of 130 fs, and repetition rate of 1 kHz. The laser beam ($P \approx 810$ mW) was focused using an aspheric lens of $f = 150$ mm to the elliptical area of

https://dx.doi.org/10.1021/acs.cgd.0c00260
Cryst. Growth Des. 2020, 20, 4454−4460

approximately 0.5 cm^2 and was directed onto samples at 45 deg. Signal-collecting optics, mounted to the glass optical fiber, was placed perpendicularly to the plane of sample (backscattering geometry). Scattered pumping radiation was suppressed with the use of 700 nm short-pass dielectric filter (FESH0700, Thorlabs). The spectra of the diffused SHG were recorded by an Ocean Optics 2000 fiber-coupled CCD spectrograph. The collection time of SHG traces for both, struvite and KDP, was 7000 ms.

2.4. Imaging Method of Ferroelectric Domains. To visualize the domains, measurements of birefringence were made by means of an Oxford Cryosystems Metripol Birefringence Imaging System (Metripol). Details of the technique have been described elsewhere.[35−37] Hence, we give here only a short description of the experimental technique. The hot stage was capable of maintaining a constant temperature to within 0.1 K. The Metripol system consists of a polarizing microscope equipped with a computer-controlled plane-polarizer capable of being rotated to fixed angles α from a reference position, a circularly polarizing analyzer, and a CCD camera. The intensity measured at any position within the captured image is given by the formula $I = I_0/2\cdot[1 + \sin(2\varphi - 2\alpha)\sin\delta]$, where I_0 is the intensity of light passed through the sample and represents its transmittance, φ is the angle of an axis of the optical indicatrix of the specimen projected onto the image measured from a predetermined direction (it is measured anticlockwise from the horizontal axis), and δ is the phase difference between the polarized light components and is given by $\delta = 2\pi\lambda^{-1}(n_1 - n_2)d$, where λ is the wavelength of the light, d is the thickness of the sample, and $\Delta n = (n_1 - n_2)$ is the so-called plano-birefringence of the sample, i.e., the birefringence measured as seen in projection down the microscope axis. By measuring several images with varying angle α between polarizer and analizer, the quantities $|\sin\delta|$ and φ are separately calculated, and then images of these quantities are shown in false color techniques. In this way, any spatial variation in the birefringence or orientation can be presented with a very high sensitivity. It is an original technique for checking the optical anisotropy of the crystal.

3. RESULTS

Using the single diffusion gel growth technique described in Materials and Methods, struvite crystals were obtained in the form of rectangular plates with the largest dimension along the b axis of up to 1 cm. An exemplary photo of such a crystal is shown in Figure 1.

Struvite structure was examined several times using single X-ray diffraction[31,38−40] and neutron diffraction.[41] These studies show that struvite crystallizes in the orthorhombic non-centrosymmetric polar space group $Pmn2_1$ (No. 31). The point group is $mm2$, and the unit cell parameters are as follows: a = 6.9650(2) Å, b = 6.1165(2) Å, and c = 11.2056(3) Å.[31] These results indicate that struvite exhibits symmetry that allows for the existence of the ferroelectric phenomenon. However, to make sure that struvite is indeed non-centrosymmetric, we have checked whether struvite generates the second harmonic of radiation upon irradiation with femtosecond laser pulses, since observation of SHG is possible only in materials of acentric structure.

To that end, the Kurtz−Perry powder test was performed.[33] The irradiation of size-graded powder of struvite (125−177 μm) with 800 nm femtosecond laser pulses at 293 K gave a clear SHG signal (Figure 2, red trace), providing strong evidence for the non-centrosymmetric nature of this compound. Under identical irradiation conditions, the SHG signal from reference KDP powder of the same particle size distribution was collected (Figure 2, black trace). The ratio of integral intensities of SHG signals ($I_{struvite}/I_{KDP}$) shows that struvite offers an SHG response as high as 0.36 that of KDP at

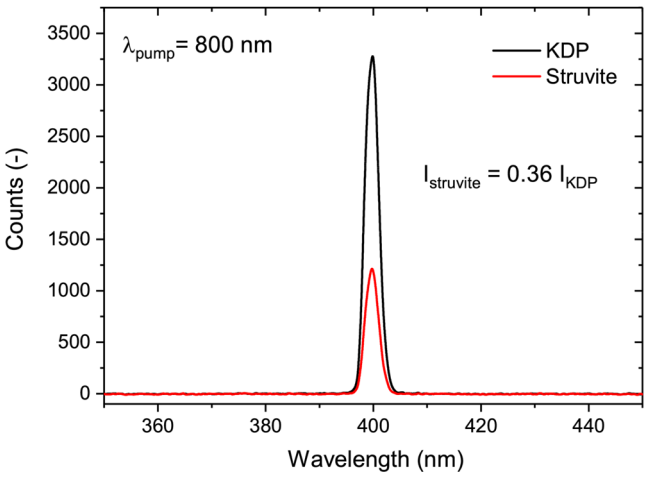

Figure 2. A comparison of SHG traces for struvite (red) and that of KDP (black).

room temperature; hence this material is strongly polar at ambient conditions.

We also carried out a detailed study on the dielectric properties of struvite. The study of the dielectric properties was performed on several struvite single crystals properly prepared as reported in Materials and Methods. At 1 kHz, the compound showed few leakage current losses with an average relative permittivity $\varepsilon_R = 50 \pm 4$, behaving as a good dielectric material between 0.1 kHz and 1 kHz for pulses of variable amplitude 20−1200 V. The dynamics of the dielectric response was studied as a function of the duration of the pulse under low-voltage excitations, and it is plotted in Figure 3.

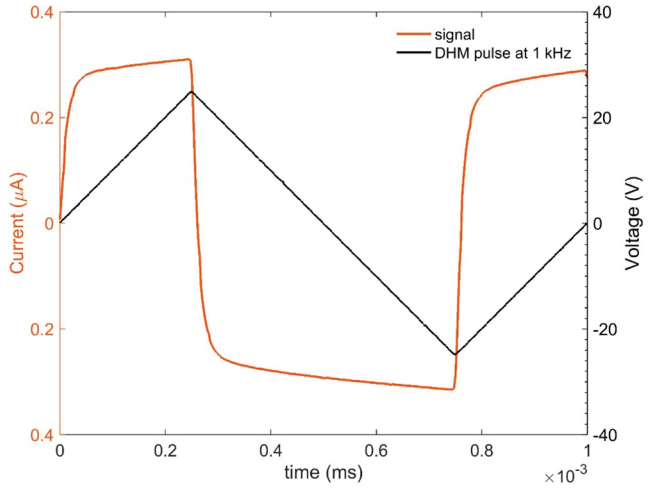

Figure 3. DHM measurement performed at 1 kHz on a planar plate capacitor with struvite as the dielectric component in the low-voltage regime.

The plot highlights the phase retardation of the current signal (orange curve of Figure 3) with respect to the linear voltage excitation, displaying in the characteristic charging and discharging mechanism of the capacitor ruled by an exponential law $I(t) = I_0 e^{-t/\tau}$, with a characteristic constant time $\tau = RC$ (where R is the equivalent circuit resistance). Noteworthy, the sign of this current depends on the first derivative sign of the triangle voltage pulse. Moreover, following the law for a purely capacitive electronic circuit:

https://dx.doi.org/10.1021/acs.cgd.0c00260
Cryst. Growth Des. 2020, 20, 4454−4460

$$Q(t) = CV(t) \quad (1)$$

where C is the capacitance of the circuit, Q is the electric charge gathered on the capacitor plates, and V is the potential difference across the capacitor.

If $V(t)$ is linearly dependent versus t, as in the case of a triangle bias, the current intensity $I(t)$

$$I(t) = \mathrm{d}Q(t)/\mathrm{d}t \propto C \quad (2)$$

is time-independent.

Equation 2 explains why, once the capacitor is fully charged, the current response is almost invariant as the voltage intensity is increased, confirming the almost ideal dielectric behavior of struvite (Figure 3). Considering the non-centrosymmetric nature of the struvite, the necessary condition for the existence of a polar state in the material is fulfilled. Hence, we proceeded to measure the ferroelectric phenomenon.

The ferroelectricity was measured through a DHM protocol on a sample of struvite with a thickness around 0.072 cm and surface area of 0.25 cm^2. The results, plotted in Figure 4 (blue

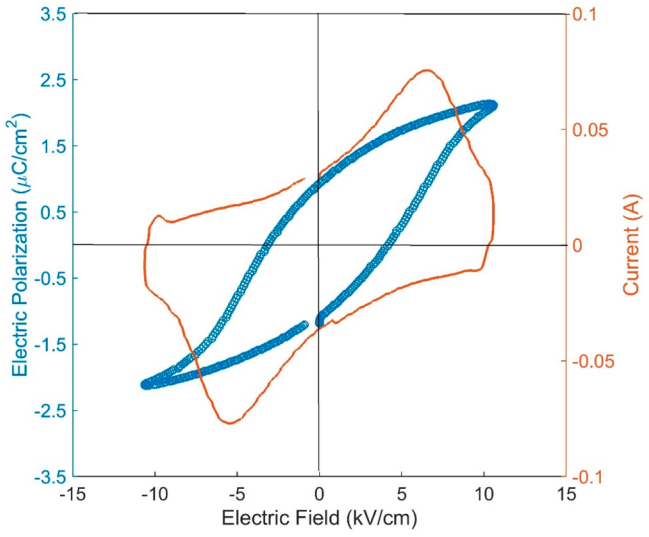

Figure 4. DHM collected on a struvite crystal in ambient conditions, applying 1 kHz triangle pulses of 1100 V voltage intensity. Polarization hysteresis loop (blue circles), current hysteresis loops (orange curve).

circles), unequivocally demonstrate that struvite is a ferroelectric material with a hysteresis loop characterized by residual polarization of about 0.95 $\mu C/cm^2$ (0.095 C/m^2) and mean coercive field of 3.7 kV/cm. Even if not saturated yet, the polarization shows a well-defined hysteretic behavior in correspondence to the polarization lobes of the integrated current (orange curve of Figure 4), ruling out possible extrinsic effects during the measurement. Since the saturation state has not been reached, the value of spontaneous polarization could not be specified. However, our measurements indicate that an intrinsic polarization definitely exists in the struvite, and its value should be close to the residual polarization value. The spontaneous polarization vector is parallel to the crystallographic z axis. The existence of spontaneous polarization means the existence of a net electric dipole resultant along the z axis.

In addition, we observed that, after a positive voltage prepoling, the following DHM triangle reading pulse detected the formation of a spontaneous positive polarization state equal to 0.45 $\mu C/cm^2$ (0.0045 C/m^2) at 0 V (see the red circle in Figure 5), confirming that it is possible to write and retain a

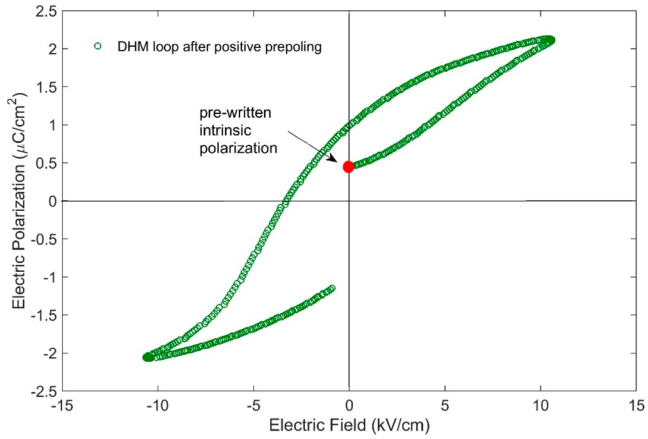

Figure 5. DHM collected with 1 kHz triangle pulses of 1100 V voltage amplitude on a virgin struvite crystal after a positive prepoling in ambient conditions.

spontaneous polarization in the struvite crystal, by inducing a preferential orientation of the electric domains in the crystal structure. This intrinsic polar state can be switched to negative with a complete triangular pulse of the proper intensity as highlighted in the green curve of Figure 5.

One of the methods used for confirming the existence of spontaneous polarization is the imaging of ferroelectric domains. An area with spontaneous polarization P_S pointing in one direction is called the ferroelectric domain. Usually, the grown crystals have a multidomain structure whose relative orientation depends on the symmetry of the crystal. It is indeed so for struvite. In Figure 6, we present the map of birefringence (Figure 6a) and map of optical indicatrix (Figure 6b) for struvite crystal at 25 °C. Light of the 570 nm wavelength was passing perpendicularly to the (001) plane (the crystal's habit is defined in Figure 7). Domains of irregular shapes and distribution of values of birefringence inside the domains characterize the complex domain structure of struvite. Birefringence distribution inside domains is most probably caused by the irregular surface of the crystal surface. On the other hand, as it is shown in Figure 6b, optical indicatrix orientations take only two values: 0° (dark magenta) and 90° (green), with an almost equal population of these two angles. These first tests of domain visualization permitted us also to evaluate the value of birefringence at room temperature on the order of 10^{-4}.

The struvite crystal morphology and habit are schematically shown in Figure 7. The number of crystalline surfaces present in the crystal may vary slightly for individual crystals (a detailed description of the morphology along with Miller indices of faces of struvite crystal growing in metasilicate gel is presented in ref 31). Figure 7 shows the struvite morphology with the largest number of faces observed. However, faces (001) and $(00\bar{1})$ relevant to spontaneous polarization always occur. The face $(00\bar{1})$ is opposite to the face (001) and is not visible in Figure 7. From the direction of the electric field applied to crystal, it was concluded that the majority of the positive ferroelectric domains are gathered on the $(00\bar{1})$ surface (Figure 5, red dot). In other words, the charge on the surface (001) is positive and on the surface (001) is negative.

https://dx.doi.org/10.1021/acs.cgd.0c00260
Cryst. Growth Des. 2020, 20, 4454−4460

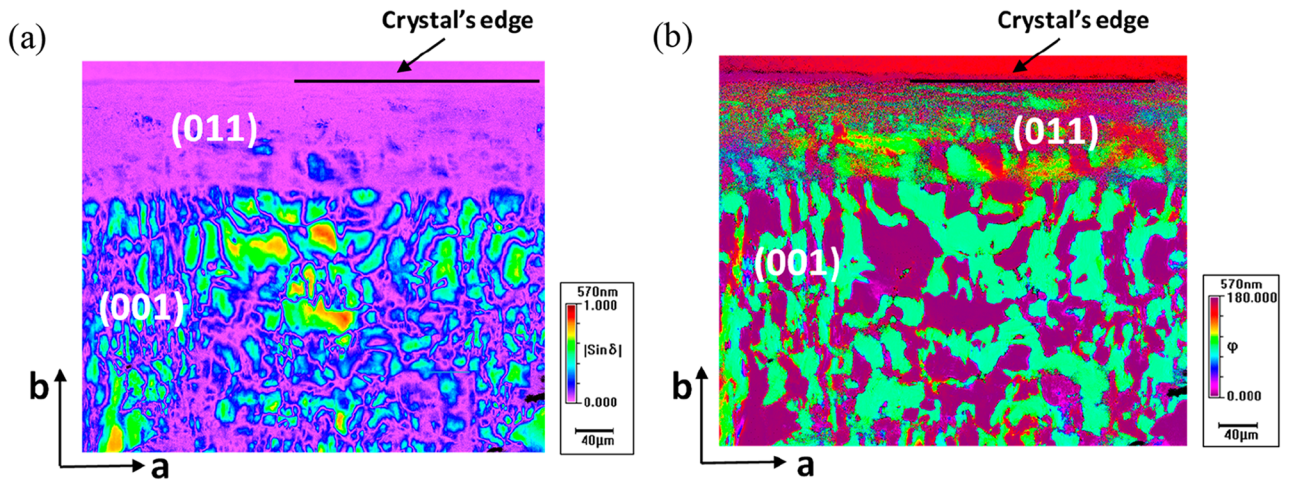

Figure 6. Maps of birefringence (a) and optical indicatrix orientations (b) at room temperature for struvite crystal of thickness 0.825 mm. Crystal habit was as that defined in Figure 7 (see (001) and (011) faces).

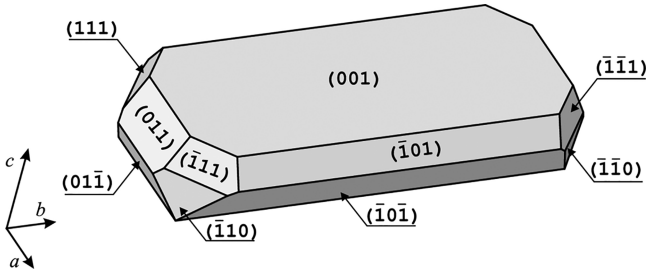

Figure 7. Schematic representation of the struvite habit with Miller indices of crystalline surfaces.

The existence of residual polarization and, as a consequence, spontaneous polarization and surface charges on the opposite struvite surfaces perpendicular to the z axis can have a significant impact on the behavior of the struvite in the urine or liquid wastewater environment. Let us consider urine, which is a very complex aqueous solution. It consists of 11 different chemical compounds,[23,28] which in turn lead to the existence in the urine of a very large amount of ions or complex chemical complexes with different electrical charges. For example, in ref 28, 60 different ions and chemical complexes are considered.

In urine, individual struvite surfaces will attract ions or chemical complexes with opposite charge signs on these surfaces. Ions or chemical complexes attracted to the surface of struvite can inhibit/promote the growth of this surface, which in turn can lead to a change in the habit of struvite. Struvite habit changes may be beneficial or not. The changes leading to a reduction in the size of struvite (growth inhibition) should be considered favorable, which as a consequence may lead to easier excretion of crystalline phases from the urinary tract. On the other hand, the surface electrical charge of struvite can also affect the zeta potential of struvite in urine. Consequently, this may affect the aggregation of struvite in urine. Aggregation of solid phases and bacteria found in urine is important in the formation of urinary stone.[41] The urinary stone is not formed because one crystal is growing, but because the aggregation of a large number of small crystals, amorphous phases, bacteria, and other organic phases that may originate, for example, from the exfoliative cells of the urinary tract. This is because aggregation is a much faster process than single crystal growth.[42,43] The electric charge accumulated on opposite planes of the struvite may also affect the capture of admixtures, especially those with electric charge. This phenomenon can also affect the modification of the struvite habit.

Surface electrical charge of struvite can also affect bacterial adhesion. It can be different on different struvite crystal surfaces. It is known that the bacteria *Proteus mirabilis*, which are most often isolated from infectious urinary stones, show a negative zeta potential, ζ, approximately equal to −30 mV regardless of urine pH.[44] This means that these bacteria due to van der Waals interactions should be more effectively attracted to the surface $(00\bar{1})$ that has a positive charge.

The reasoning carried out shows that the ferroelectric properties of struvite, in particular, spontaneous polarization, can have a significant impact on the course of physicochemical processes occurring in urine. It seems that the ferroelectric properties of struvite may also have a significant impact on processes in liquid wastewater.

One may wonder what the order of magnitude of spontaneous polarization is for various minerals. However, it should be noted that, as explained above, we can only compare the residual polarization of struvite with the spontaneous polarization of other minerals. In a review article,[7] the spontaneous polarization values for several ferroelectric minerals are given. The smallest spontaneous polarization value equal to 0.00012 C/m^2 is given for the pyrolusite mineral.[7] The highest values of spontaneous polarization occur for minerals such as heftetjernite (0.5 C/m^2 at −35 °C), macedonite (from 0.4 to 0.8 C/m^2 depending on the temperature[7]), and barioperovskite (0.2 C/m^2 for temperature equal and lower than 135 °C). There are also minerals with values of spontaneous polarization between the lowest and highest values and minerals with values of spontaneous polarization of the same order of magnitude as the residual polarization measured by us for struvite. For example, for gwihabaite, spontaneous polarization is 0.007 C/m^2 at 120 °C) and for boraciteitis is 0.008C/m^2 at 267 °C.[7]

4. CONCLUSIONS

Our research presented in this article indicates that struvite meets all fundamental requirements necessary to be considered as a ferroelectric crystal. Struvite exhibits a hysteresis loop with a residual polarization of about 0.95 μC/cm^2 (0.095 C/m^2)

https://dx.doi.org/10.1021/acs.cgd.0c00260
Cryst. Growth Des. 2020, 20, 4454−4460

and a mean coercive field of 3.7 kV/cm. The spontaneous polarization vector is parallel to the crystallographic axis z, which means the existence of a net electric dipole along this axis. Ferroelectric domains associated with spontaneous polarization were visualized using birefringence imaging techniques. Two types of ferroelectric domain configurations (0° and 90° types) were observed in struvite. The research also allowed to determine the value of birefringence of struvite at room temperature, which is on the order of 10^{-4}. Ferroelectric properties of struvite, in particular, electric spontaneous polarization, can have a significant impact on the behavior of struvite in aqueous solutions, such as liquid wastewater or urine. The electric charge accumulated on the opposite struvite surfaces perpendicular to the crystallographic axis z and resulting from the existence of spontaneous polarization may affect the capture of admixtures, especially those with electric charge, i.e., ions. As a consequence, this can lead to a change in the morphology and habit of these crystals. The surface charge of struvite can also affect bacterial adhesion (in urine in the case of infection) as well as aggregation of struvite crystals with each other as well as with bacteria.

Although struvite is a mineral known since 1845, characterization of its ferroelectric properties is presented for the first time in this article. This coincides with the 100th anniversary of the discovery of ferroelectricity.

AUTHOR INFORMATION

Corresponding Author

Jolanta Prywer − *Institute of Physics, Lodz University of Technology, 90-924 Łódź, Poland;* orcid.org/0000-0001-5161-2785; Email: jolanta.prywer@p.lodz.pl

Authors

Davide Delmonte − *Institute of Materials for Electronics and Magnetism (IMEM), CNR, Parma, Italy*

Massimo Solzi − *Department of Mathematical, Physical and Computer Sciences, the University of Parma, Parma, Italy*

Francesco Cugini − *Department of Mathematical, Physical and Computer Sciences, the University of Parma, Parma, Italy*

Krystian Roleder − *Institute of Physics, University of Silesia, 41-500 Chorzów, Poland*

Andrzej Soszyński − *Institute of Physics, University of Silesia, 41-500 Chorzów, Poland*

Agnieszka Ciżman − *Department of Experimental Physics, Wroclaw University of Science and Technology, 50-370 Wroclaw, Poland;* orcid.org/0000-0002-8906-4080

Jan K. Zaręba − *Advanced Materials Engineering and Modelling Group, Wroclaw University of Science and Technology, 50-370 Wroclaw, Poland;* orcid.org/0000-0001-6117-6876

Complete contact information is available at: https://pubs.acs.org/10.1021/acs.cgd.0c00260

Author Contributions

J.P. formulated the problem raised in the article, managed a research project covering research that is the problem of the article, and has grown struvite crystals using a single diffusion gel growth technique. D.D. and F.C. prepared the electrical bonding, measured the dielectric properties, and measured the hysteresis loop by DHM protocol. D.D., F.C., and M.S. analyzed the polarization data and verified that spontaneous polarization can be reversed by an application of an external electric field. K.R. and A.S. visualized ferroelectric domains using birefringence imaging techniques. J.Z. and A.C., using the SHG method, showed that struvite is non-centrosymmetric. All the authors took part in writing the manuscript.

Funding

This work was supported by the Ministry of Science and Higher Education (Poland), Grant No. I-71/501/7-71-1-1.

Notes

The authors declare no competing financial interest.

ACKNOWLEDGMENTS

J.P. and D.D. would like to thank Professor Roberto Fornari (University of Parma, Italy) who put them in contact.

REFERENCES

(1) Valasek, J. Piezoelectric and allied phenomena in Rochelle salt. *Phys. Rev.* **1921**, *17*, 475−481.

(2) Valasek, J. Piezo-Electric and Allied Phenomena in Rochelle Salt. *Phys. Rev.* **1921**, *17*, 475−481.

(3) Fousek, J. Joseph Valasek and the discovery of ferroelectricity. *Proceedings of 1994 IEEE International Symposium on Applications of Ferroelectrics*; University Park, PA, USA, 1994; pp 1−5.

(4) Busch, G.; Scherrer, P. Eineneue seignette-elektrische Substanz. *Naturwissenschaften* **1935**, *23*, 737−737.

(5) Matthias, B.; von Hippel, A. Domain Structure and Dielectric Response of Barium Titanate Single Crystals. *Phys. Rev.* **1948**, *73*, 1378−1384.

(6) Soergel, E. Visualization of ferroelectric domains in bulk single crystals. *Appl. Phys. B: Lasers Opt.* **2005**, *81*, 729−752.

(7) Helman, D. S. Symmetry-based electricity in minerals and rocks: A review with examples of centrosymmetric minerals that exhibit pyro and piezoelectricity. *Periodico di Mineralogia* **2016**, *85*, 201−248.

(8) Landau, L. D. On the Theory of Phase Transitions. *Phys. Z. Sowjet.* **1937**, *11*, 26. See also *Collected Papers of L. D. Landau*; Ter-Haar, D., Ed.; Pergamon, 1965; pp 193−216.

(9) Ulex, G. L. On struvite, a new mineral. *Mem. Proc. Chem. Soc.* **1845**, *3*, 106−110.

(10) Lafuente, B.; R. T., Downs, Yang, H.; Stone, N. The power of databases: The RRUFF project. In *Highlights in Mineralogical Crystallography*; Armbruster, T.; Danisi, R.M., Eds.; W. De Gruyter: Berlin, Germany, 2015; pp 1−30. Available online: http://rruff.geo.arizona.edu/doclib/hom/struvite.pdf (accessed on 12 November 2019).

(11) Doyle, J. D; Parsons, S. A Struvite formation, control and recovery. *Water Res.* **2002**, *36*, 3925−3940.

(12) Brett, S.; Guy, J.; Morse, G. K.; Lester, J. N. *Phosphorous Removal and Recovery Technologies*; Selper Publications, London, 1997.

(13) Booker, N. A.; Priestley, A. J.; Fraser, I. H. Struvite formation in wastewater treatment plants: Opportunities for nutrient recovery. *Environ. Technol.* **1999**, *20*, 777−782.

(14) Jaffer, Y; Clark, T.A; Pearce, P; Parsons, S.A Potential phosphorous recovery by struvite formation. *Water Res.* **2002**, *36*, 1834−1842.

(15) Maqueda, C.; Perez Rodriguez, J. L.; Lebrato, J. Study of struvite precipitation in anaerobic digesters. *Water Res.* **1994**, *28*, 411−416.

(16) Ghos, G.; Mohan, K.; Sarkar, A. Struvite proves a good fertilizer. *CEEP Scope Newslett.* **2002**, *37*, 3−4.

(17) Gaterell, M. R.; Gay, R.; Wilson, R.; Gochin, R. J.; Lester, J. N. An economic and environmental evaluation of the opportunities for substituting phosphorus recovered from wastewater treatment works in existing UK fertiliser markets. *Environ. Technol.* **2000**, *21*, 1067−1084.

(18) Weil, M. The struvite-type compounds $M[Mg(H_2O)_6](XO_4)$, where M = Rb, Tl and X = P. *Cryst. Res. Technol.* **2008**, *43*, 1286−1291.

(19) Strickland, J. Perspectives for phosphorous recovery offered by enhanced biological removal. *Environ. Technol.* **1999**, *20*, 721−725.

https://dx.doi.org/10.1021/acs.cgd.0c00260
Cryst. Growth Des. 2020, 20, 4454−4460

(20) Abbona, F.; Franchini-Angela, M. Crystallization of calcium and magnesium phosphates from solution of low concentration. *J. Cryst. Growth* **1990**, *104*, 661−671.
(21) Bichler, K. H.; Eipper, E.; Naber, K.; Braun, V.; Zimmermann, R.; Lahme, S. S. Urinary infection stones. *Int. J. Antimicrob. Agents* **2002**, *19*, 488−498.
(22) Gleeson, M. J.; Griffith, D. P. Struvite calculi. *Br. J. Urol.* **1993**, *71*, 503−511.
(23) Griffith, D. P.; Musher, D. M.; Itin, C. Urease. The primary cause of infection-induced urinary stones. *Invest. Urol.* **1976**, *13*, 346−350.
(24) McLean, R. J. C.; Nickel, J. C.; Cheng, K.-J.; Costerton, J. W.; Banwell, J. G. The ecology and pathogenicity of urease-producing bacteria in the urinary tract. *CRC Cr. Rev. Microbiol.* **1988**, *16*, 37−79.
(25) Leusmann, D. B.; Sabinski, F. Potential contribution of optional urease-positive bacteria to idiopathic urinary calcium stone formation. *Urol. Res.* **1996**, *24*, 73−78.
(26) Amtul, Z.; Atta-ur-Rahman; Siddiqui, R. A.; Choudhary, M. I. Chemistry and mechanism of urease inhibition. *Curr. Med. Chem.* **2002**, *9*, 1323−1348.
(27) Bouropoulos, N. Ch.; Koutsoukos, P. G. Spontaneous precipitation of struvite from aqueous solutions. *J. Cryst. Growth* **2000**, *213*, 381−388.
(28) Prywer, J.; Mielniczek-Brzóska, E. Chemical equilibria of complexes in urine. A contribution to the physicochemistry of infectious urinary stone formation. *Fluid Phase Equilib.* **2016**, *425*, 282−288.
(29) Chauhan, C. K.; Joshi, M. J. In vitro crystallization, characterization and growth inhibition study of urinary type struvite crystals. *J. Cryst. Growth* **2013**, *362*, 330−337.
(30) Website of e-medicine (Medscape): Struvite and Staghorn Calculi. http://emedicine.medscape.com/article/439127; Accessed 18 November 2019.
(31) Prywer, J.; Sieroń, L.; Czylkowska, A. Struvite grown in gel, its crystal structure at 90 K and thermoanalytical study. *Crystals* **2019**, *9*, 89.
(32) Delmonte, D.; Mezzadri, F.; Gilioli, E.; Solzi, M.; Calestani, G.; Bolzoni, F.; Cabassi, R. Poling-Written Ferroelectricity in Bulk Multiferroic Double-Perovskite $BiFe_{0.5}Mn_{0.5}O_3$. *Inorg. Chem.* **2016**, *55*, 6308−6314.
(33) Kurtz, S. K.; Perry, T. T. A powder technique for the evaluation of nonlinear optical materials. *J. Appl. Phys.* **1968**, *39*, 3798−3813.
(34) Graja, A. Production of the Second Harmonic of Light in Ammonium Pentaborate and other Powdered Piezoelectric Crystals. *Phys. Status Solidi B* **1968**, *27*, K93−K97.
(35) Glazer, A. M.; Lewis, J. G.; Kaminsky, W. An Automatic Optical Imaging System for Birefringent Media. *Proc. R. Soc. London, Ser. A* **1996**, *452*, 2751.
(36) Geday, M. A.; Kaminsky, W.; Lewis, J. G.; Glazer, A. M. Images of absolute retardance L.Δn, using the rotating polariser method. *J. Microsc.* **2000**, *198*, 1−9.
(37) Geday, M. A.; Glazer, A. M. Birefringence of $SrTiO_3$ at the ferroelastic phase transition. *J. Phys.: Condens. Matter* **2004**, *16*, 3303−3310.
(38) Whitaker, A.; Jeffery, J. W. The Crystal Structure of Struvite, $MgNH_4PO_4{\cdot}6H_2O$. *Acta Crystallogr., Sect. B: Struct. Crystallogr. Cryst. Chem.* **1970**, *26*, 1429−1440.
(39) Abbona, F.; Calleri, M.; Ivaldi, G. Synthetic Struvite, $MgNH_4PO_4{\cdot}6H_2O$: Correct Polarity and Surface Features of Some Complementary Forms. *Acta Crystallogr., Sect. B: Struct. Sci.* **1984**, *40*, 223−227.
(40) Tansman, G. F.; Kindstedt, P. S.; Hughes, J. M. Minerals in Food: Crystal Structures of Ikaite and Struvite from Bacterial Smears on Washed-Rind Cheese. *Can. Mineral.* **2017**, *55*, 89−100.
(41) Ferraris, G.; Fuess, H.; Joswig, W. Neutron Diffraction Study of $MgNH_4PO_4{\cdot}6H_2O$ (Struvite) and Survey of Water Molecules Donating Short Hydrogen Bonds. *Acta Crystallogr., Sect. B: Struct. Sci.* **1986**, *42*, 253−258.
(42) Espinosa-Ortiz, E. J.; Eisner, B. H.; Lange, D.; Gerlach, R. Current insights into the mechanisms and management of infection stones. *Nat. Rev. Urol.* **2019**, *16*, 35−53.
(43) Prywer, J.; Torzewska, A. Aggregation of poorly crystalline and amorphous components of infectious urinary stones is mediated by bacterial lipopolysaccharide. *Sci. Rep.* **2019**, *9*, 17061.
(44) Prywer, J.; Sadowski, R. R.; Torzewska, A. Aggregation of Struvite, Carbonate Apatite, and Proteus mirabilis as a Key Factor of Infectious Urinary Stone Formation. *Cryst. Growth Des.* **2015**, *15*, 1446−1451.

https://dx.doi.org/10.1021/acs.cgd.0c00260
Cryst. Growth Des. 2020, 20, 4454−4460